**CMPUT 654: Mathematical Foundations of Modern AI Systems** Fall 2026

# Lecture 10: Implicit bias and solution selection

October 6, 2026

*Lecturer: Csaba Szepesvári* *Note prepared by: Csaba Szepesvári*

**Reading guide.** The empirical objective need not determine one predictor. This lecture asks what an optimization method selects among the resulting possibilities. The main text follows the development in class. We first distinguish non-uniqueness of parameters from non-uniqueness of the represented model. We then pay a debt from Lecture 9 by proving that zero-initialized gradient descent selects the minimum-Euclidean-norm least-squares interpolant. The central case is linear logistic classification on separable data: gradient descent and signed gradient descent select different max-margin directions, and either direction can have smaller population classification risk. We prove the continuous-time steepest-descent result used to explain this selection, discuss the two regimes of Adam, and finish the main exposition with the distinction between constant and decreasing stepsizes under different sources of gradient noise. Material not reached in class is marked with $^*$. The supplementary material treats early stopping as a spectral filter, the construction of Wilson et al. [2017], noise-induced selection in neural networks, and parameter-space flatness. The prerequisites are linear algebra, least squares, and elementary probability.

## 10.1 When empirical fit does not determine the predictor

Let $f_w$ denote the predictor represented by a parameter vector $w$, and let $L_n(w)$ be its empirical training loss. If $L_n$ has many minimizers, two different kinds of non-uniqueness must be separated.

**Definition 10.1.1** (Parameter and model non-uniqueness)**.** There is *parameter-space non-uniqueness* when distinct parameters $w \neq w'$ both minimize the empirical loss. There is *model non-uniqueness* when empirical minimizers represent predictors that differ on some input: $f_w \neq f_{w'}$.

Parameter-space non-uniqueness need not produce model non-uniqueness. In a neural network, permuting hidden units can leave the represented function unchanged. For a positively homogeneous unit, the rescaling

$$a[b^\top x]_+ = \frac{a}{c}[(cb)^\top x]_+, \qquad c > 0,$$

also changes the parameters without changing the predictor. Such parameter symmetries matter when discussing optimization paths or parameter-space curvature, but the symmetries do not by themselves change a prediction. The statistical issue in this lecture is model non-uniqueness: different empirical minimizers or limiting directions can extrapolate differently beyond the training sample.

Overparameterization makes underdetermination common. In linear regression, the data can constrain only the component of a parameter in the span of the training inputs. In a neural network, there may be many more degrees of freedom than empirical constraints. Once the empirical objective leaves a choice, the optimization procedure can do more than merely reduce the objective: the procedure's initialization, update rule, and stopping time can select among the empirically equivalent alternatives.

**Definition 10.1.2** (Explicit regularization and implicit bias)**.** A *regularizer* is an auxiliary parameter- or predictor-dependent criterion $\Omega(w)$ used to prefer some fits to others. The preference is *explicit* when training minimizes, for example,

$$L_n(w) + \lambda\Omega(w) \qquad \text{or imposes} \qquad \Omega(w) \le r.$$

The *implicit bias* of an optimization procedure is a preference induced by its initialization, update geometry, or stopping rule while the model and empirical objective are held fixed. In this lecture, *algorithmic bias* refers to this optimizer-induced selection.

The classical origin of regularization is statistical. In a rich nonparametric class, exact empirical fitting can reproduce noise or behave irregularly between observed inputs. One therefore adds a complexity or roughness penalty, such as

$$\widehat{f}_\lambda \in \arg\min_{f\in\mathcal{F}} \left\{ \frac{1}{n}\sum_{i=1}^{n}\big(Y_i - f(X_i)\big)^2 + \lambda J(f) \right\}. \tag{10.1}$$

The strength $\lambda$ may be chosen from the data, and in asymptotic analyses $\lambda$ commonly decreases with $n$. Implicit bias is surprising because a choice of optimizer can create a preference resembling regularization without adding the term $\lambda J$ to the empirical objective.

Population performance remains the criterion for deciding whether the preference is useful. If the training sample is random with law $P$, write

$$R_P(w) = \mathbb{E}_P[\ell_{\text{eval}}(w;\,\cdot)]$$

for the population risk. The evaluation loss may differ from the empirical training loss. When the optimizer itself adds bias, the main question is whether the induced bias decreases the population risk. Computational efficiency—using less computation to reach a given empirical loss, or reaching a smaller empirical loss within a fixed computational budget—also matters, but downstream performance is the criterion studied here.

We analyze the relation between optimizer-induced bias and population risk in two linear cases.

## 10.2 Least squares: initialization determines the invisible component

Consider linear least squares when the number of parameters is greater than the number of datapoints. The minimizer of the loss is not unique: Any interpolating solution leads to zero (minimum) loss, and there are many such solutions.

Lecture 9 motivated minimum-norm interpolation by stating that gradient descent has an algorithmic bias toward a minimum-norm solution. Lecture 9 also studied the downstream consequences and found that the usefulness of this bias depends on the choice and scaling of features. We now prove the selection claim about gradient descent.

To prove this selection claim, fix $x_1, \ldots, x_n \in \mathbb{R}^d$ and $y_1, \ldots, y_n \in \mathbb{R}$, and define the *data span*

$$\mathcal{R} = \operatorname{span}\{x_1, \ldots, x_n\} \subseteq \mathbb{R}^d.$$

The data span $\mathcal{R}$ is a linear subspace of $\mathbb{R}^d$. When there are more parameters than datapoints ($d > n$), i.e., in the overparametrized regime, $\mathcal{R}$ is a nontrivial subspace of $\mathbb{R}^d$; that is, $\mathcal{R} \neq \mathbb{R}^d$. The

orthogonal complement of the data span is

$$\mathcal{R}^\perp = \{v \in \mathbb{R}^d : \langle v, x_i \rangle = 0 \text{ for every } i \in [n]\}.$$

Predictions take the form $x \mapsto \langle x, w \rangle$ where $w \in \mathbb{R}^d$ is a model parameter. Let $f_w(x) = \langle x, w \rangle$. The data cannot distinguish $w$ from $w + v$ when $v \in \mathcal{R}^\perp$ in the sense that $f_w(x_i) = f_{w+v}(x_i)$ for all $i \in [n]$ for any $w \in \mathbb{R}^d$ and $v \in \mathcal{R}^\perp$.

Consider

$$L_n(w) = \frac{1}{2} \sum_{i=1}^{n} \big(\langle w, x_i \rangle - y_i\big)^2. \tag{10.2}$$

The gradient equation

$$\nabla L_n(w) = \sum_{i=1}^{n} \big(\langle w, x_i \rangle - y_i\big) x_i = 0 \tag{10.3}$$

is called the *normal equation*. To write it in matrix form, let $\mathbf{X} \in \mathbb{R}^{n \times d}$ have row $i$ equal to $x_i^\top$, and let $y = (y_1, \ldots, y_n)^\top$. Then

$$\nabla L_n(w) = \mathbf{X}^\top (\mathbf{X} w - y).$$

Assume

$$\dim(\mathcal{R}) = n. \tag{10.4}$$

The rank theorem says that condition Eq. (10.4) is equivalent to $\mathbf{X}\mathbf{X}^\top$ being nonsingular. The rank theorem also implies that $\mathbf{X} : \mathbb{R}^d \to \mathbb{R}^n$ is onto. Consequently, arbitrary responses $y \in \mathbb{R}^n$ can be interpolated. Moreover, $\mathbf{X}^\top$ is one-to-one, so the normal equation is equivalent to

$$\mathbf{X} w = y. \tag{10.5}$$

Thus every minimizer interpolates and has loss zero. Conversely, every interpolant has loss zero and is therefore a minimizer.

Define

$$w^\star = \mathbf{X}^\top (\mathbf{X}\mathbf{X}^\top)^{-1} y. \tag{10.6}$$

Substitution gives $\mathbf{X} w^\star = y$, and $w^\star \in \mathcal{R}$ because $w^\star$ is a linear combination of the $x_i$.

**Proposition 10.2.1** (Initialization determines the least-squares interpolant)**.** *Every minimizer of Eq. (10.2) has the unique form*

$$w^\star + v, \qquad v \in \mathcal{R}^\perp.$$

*The vector $w^\star$ is the unique minimum-Euclidean-norm minimizer. Furthermore, consider gradient descent*

$$w_{t+1} = w_t - \eta \sum_{i=1}^{n} \big(\langle w_t, x_i \rangle - y_i\big) x_i, \qquad 0 < \eta < \frac{2}{\|\mathbf{X}\|_{\mathrm{op}}^2}. \tag{10.7}$$

*If $v_0$ is the orthogonal projection of $w_0$ onto $\mathcal{R}^\perp$, then*

$$w_t \longrightarrow w^\star + v_0.$$

*In particular, $w_0 = 0$ selects $w^\star$.*

*Proof.* If $w$ is a minimizer, then Eq. (10.5) and $\mathbf{X}w^\star = y$ give

$$\langle w - w^\star, x_i \rangle = 0 \qquad (i \in [n]).$$

Hence $w - w^\star \in \mathcal{R}^\perp$. Conversely, $\mathbf{X}(w^\star + v) = y$ for every $v \in \mathcal{R}^\perp$, proving the claimed description of all minimizers. Since $w^\star \in \mathcal{R}$ and $v \in \mathcal{R}^\perp$, the Pythagorean theorem gives

$$\|w^\star + v\|_2^2 = \|w^\star\|_2^2 + \|v\|_2^2.$$

Therefore $w^\star$ is the unique minimum-norm minimizer.

Every increment $w_{t+1} - w_t$ in Eq. (10.7) is a linear combination of the $x_i$ and hence belongs to $\mathcal{R}$. The component of $w_t$ in $\mathcal{R}^\perp$ therefore remains equal to $v_0$. Write $w_t = r_t + v_0$ with $r_t \in \mathcal{R}$. Since $\mathbf{X}v_0 = 0$ and $\mathbf{X}w^\star = y$,

$$r_{t+1} - w^\star = \big(I - \eta \mathbf{X}^\top \mathbf{X}\big)(r_t - w^\star).$$

The restriction of $\mathbf{X}^\top \mathbf{X}$ to $\mathcal{R}$ is positive definite. The eigenvalues of this restriction lie in $(0, \|\mathbf{X}\|_{\mathrm{op}}^2]$, so the stepsize assumption makes the last linear map a strict contraction on every eigendirection in $\mathcal{R}$. Thus $r_t \to w^\star$ and $w_t \to w^\star + v_0$. □

The argument separates what the data determine from what initialization supplies. The rank assumption guarantees that the observed responses can be fit. The orthogonal decomposition says that the data constrain the component in $\mathcal{R}$ and cannot see the component in $\mathcal{R}^\perp$. Zero initialization sets that invisible component to zero, and gradients cannot create it. Exercise 1 asks you to reconstruct the argument and to show explicitly why another initialization need not select the minimum-norm solution.

## 10.3 Logistic classification on separable data

Lecture 1 introduced logits and the softmax map that converts an LLM's output scores into next-token probabilities. Training uses token log loss, whereas many deployment criteria record a discrete event such as whether the final answer is correct. The binary linear logistic model is the smallest model that retains the distinction between training and deployment losses. The binary model lets us study how a smooth probabilistic training objective can produce a sharp discrete prediction and how the optimizer can affect that prediction on unseen inputs. The binary linear model does not describe the full computation performed by a transformer.

The linear score

$$s_w(x) = \langle w, x \rangle$$

is a *logit*. The sigmoid function and the resulting conditional probability model are

$$\sigma(s) = \frac{1}{1 + e^{-s}}, \qquad q_w(y \mid x) = \sigma\big(y s_w(x)\big), \qquad y \in \{-1, 1\}.$$

The identity $\sigma(s) + \sigma(-s) = 1$ makes $q_w(\cdot \mid x)$ a probability mass function, and

$$\log \frac{q_w(1 \mid x)}{q_w(-1 \mid x)} = s_w(x).$$

Thus the log-odds are linear in $x$. The log-odds identity explains the name *logistic regression* in two parts. "Logistic" refers to the logistic link $p = \sigma(s)$ that converts a score into a probability.

"Regression" refers to modeling a conditional mean as a function of the input. Indeed, for $B = (Y+1)/2 \in \{0,1\}$,

$$\mathbb{E}[B \mid X = x] = \mathbb{P}(Y = 1 \mid X = x) \approx q_w(1 \mid x) = \sigma(\langle w, x\rangle).$$

Thus logistic regression models the conditional mean of a binary response, equivalently its success probability, through linear log-odds. Thresholding that fitted probability at $1/2$ turns the model into a classifier.

The negative log-likelihood of a labeled example is

$$-\log q_w(y \mid x) = \log\bigl(1 + e^{-y s_w(x)}\bigr).$$

Fix training examples $(x_1, y_1), \dots, (x_n, y_n) \in \mathbb{R}^d \times \{-1, 1\}$. Training minimizes the empirical logistic loss

$$L_n(w) = \frac{1}{n}\sum_{i=1}^{n} \log\bigl(1 + \exp(-y_i\langle w, x_i\rangle)\bigr). \tag{10.8}$$

At deployment, the predicted label is $h_w(x) = \operatorname{sign}(s_w(x))$, with $\operatorname{sign}(0) = 1$. If $(X, Y)$ has law $P$, the population classification risk is

$$R_P(w) = \mathbb{P}\bigl(h_w(X) \neq Y\bigr), \tag{10.9}$$

The smooth logistic loss is therefore a *surrogate loss*: a tractable training loss used in place of the deployment loss $\mathbb{I}\{h_w(x) \neq y\}$. Log loss is a *strictly proper scoring rule*: for each input $x$, its conditional expectation is uniquely minimized by predicting the true value of $\mathbb{P}(Y = 1 \mid X = x)$. This proper-scoring property is why probability fitting, rather than classification alone, explains the word "regression." Lecture 1 introduced the binary logit as log-odds, while Lecture 3 introduced sigmoid probabilities and log-loss fitting. The following review combines those ideas for a linear score. Exercise 2 asks you to derive the identities and use them to explain the name logistic regression.

More generally, a *margin loss* has the form $\ell(m)$, where $m = y s_w(x)$ is the signed margin. Common examples are

$$\ell_{\log}(m) = \log(1 + e^{-m}), \qquad \ell_{\exp}(m) = e^{-m}, \qquad \ell_{\text{hinge}}(m) = (1 - m)_+.$$

These losses decrease as the signed margin increases, but the name "margin loss" alone does not determine a probability model or an implicit bias. The tail of $\ell$ and the update geometry both affect the limiting direction. We analyze logistic loss below.

Write

$$z_i = y_i x_i$$

for the *signed feature vector*. The loss depends on $(x_i, y_i)$ only through $z_i$:

$$\log\bigl(1 + e^{-y_i\langle w, x_i\rangle}\bigr) = \log\bigl(1 + e^{-\langle w, z_i\rangle}\bigr).$$

In particular, $(x_i, y_i)$ and $(-x_i, -y_i)$ have exactly the same effect on the empirical loss. A finite training sample is *linearly separable* if some $w$ satisfies

$$\langle w, z_i\rangle > 0 \qquad \text{for every } i \in [n]. \tag{10.10}$$

The term "linearly separable" here refers to the observed sample, not automatically to the population law. On a separable sample, scaling such a $w$ drives Eq. (10.8) to zero. No finite vector attains zero, so the relevant selected object is a direction.

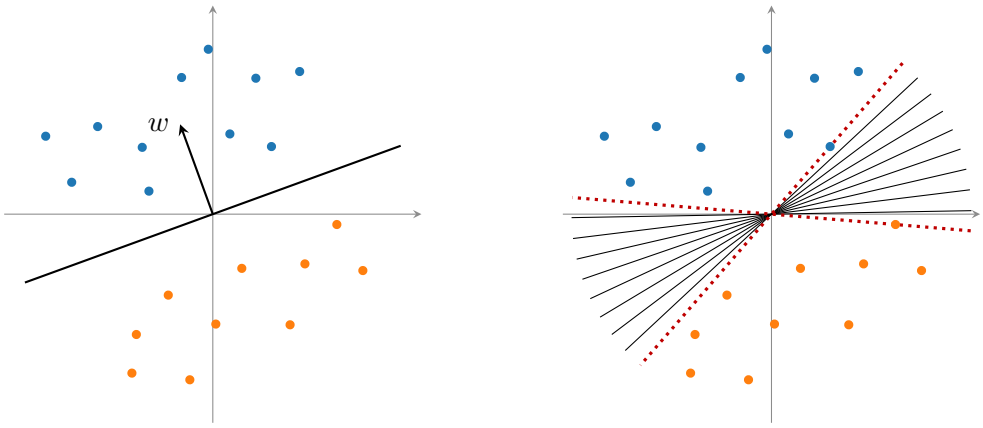



Figure 1: One separating hyperplane (left) and several of the separating hyperplanes for the same sample (right). The dotted boundary lines touch a data point and therefore do not strictly separate the sample.

Separability is an idealized property of the data at hand. A high-dimensional finite sample can be separable even when the population contains label noise. The max-margin asymptotics below describe training only while the separable model remains appropriate; they should not be applied automatically to a nonseparable or continually changing dataset.

Two discrete algorithms will be compared. With $g_t = \nabla L_n(w_t)$, ordinary gradient descent and signed gradient descent use

$$w_{t+1} = w_t - \eta_t g_t, \tag{10.11}$$

$$w_{t+1} = w_t - \eta_t \operatorname{sign}(g_t), \tag{10.12}$$

respectively. The sign is applied coordinatewise. Both methods can drive the empirical loss toward zero, but they need not approach the same direction.

For $p \in [1, \infty]$, define the *normalized empirical margin*

$$\gamma_p(w) = \frac{\min_{i\in[n]} \langle w, z_i \rangle}{\|w\|_p}, \qquad w \neq 0.$$

The normalized margin $\gamma_p(w)$ is unchanged when $w$ is multiplied by a positive scalar, so $\gamma_p(w)$ depends only on the direction of the parameter vector $w$. The norm used for normalization is a choice. At this point there is no reason internal to logistic loss to select $p = 2$, $p = \infty$, or another value. We keep $p$ explicit because two choices will arise naturally from two optimization methods.

Maximizing $\gamma_p$ is equivalent, after rescaling the smallest margin to one, to the hard-margin problem

$$\min_w \|w\|_p \quad \text{subject to} \quad \langle w, z_i \rangle \geq 1 \quad (i \in [n]). \tag{10.13}$$

Thus varying $p$ in Eq. (10.13) gives a family of norm-constrained optimization problems. A solution of each problem determines a separating direction, and the optimizer can select among these directions.

**Theorem 10.3.1** (Gradient and signed gradient descent select norm-dependent margins)**.** *Fix a linearly separable sample.*

*(a) For a sufficiently small constant stepsize, the gradient-descent iterates in Eq. (10.11) satisfy $\gamma_2(w_t) \longrightarrow \gamma_2^\star$. If the maximum-$\ell_2$-margin direction is unique, then the normalized iterates converge to that direction.*

*(b) Suppose the signed-gradient stepsizes in Eq. (10.12) are positive and nonincreasing, with* $\eta_t \longrightarrow 0$, $\sum_{t=0}^{\infty} \eta_t = \infty$. *Then*

$$\gamma_\infty(w_t) \longrightarrow \gamma_\infty^\star.$$

*If the maximum-*$\ell_\infty$*-margin direction is unique, then the normalized iterates converge to that direction.*

The stepsize assumptions are algorithm-specific. Gradient descent scales its step by the magnitude of the gradient, whereas signed descent takes a unit $\ell_\infty$ direction before applying $\eta_t$. The theorem says that gradient descent prefers Euclidean geometry, while signed descent prefers max-norm geometry. The theorem does not determine which preference has smaller population risk. Sections 10.5 and 10.6 give distributions on which either ordering occurs.

The conditions on $\eta_t$ are not cosmetic. On separable data the parameter norm must diverge, while the logistic gradient becomes exponentially small in the margins. A stepsize that decreases too quickly can leave insufficient cumulative movement. Conversely, more aggressive and even increasing stepsizes are possible for some algorithms and losses, but require a separate analysis of the discretization error.

## 10.4 Why steepest descent selects a margin geometry

Why do the two algorithms in Theorem 10.3.1 select different max-margin geometries? They measure the size of an update in different norms. The steepest-descent formulation makes the difference between the two update geometries explicit.

To see the connection before stating the theorem, let $q$ be the Hölder conjugate of $p$, so $1/p + 1/q = 1$, and let $g \neq 0$ be a gradient. A *unit steepest-descent direction* measured in $\|\cdot\|_p$ is

$$s_p(g) \in \operatorname*{arg\,min}_{\|v\|_p=1} \langle g, v \rangle. \tag{10.14}$$

Thus one unit of movement is charged according to the $\ell_p$ norm. Hölder's inequality and Eq. (10.14) give

$$\|s_p(g)\|_p = 1, \qquad \langle -g, s_p(g) \rangle = \|g\|_q. \tag{10.15}$$

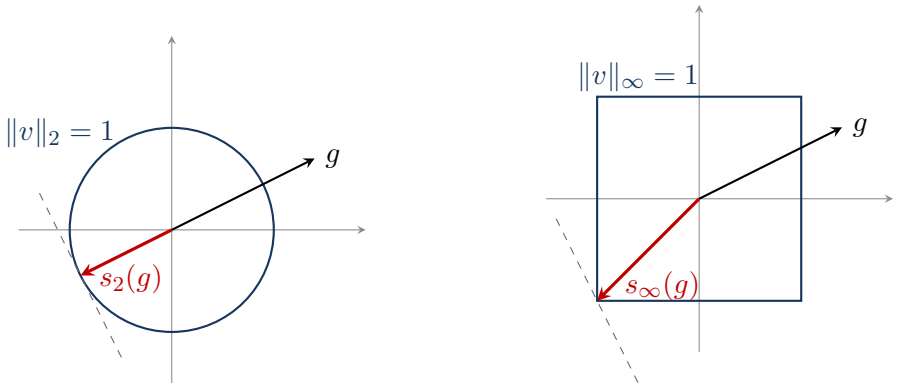



Figure 2: The unit steepest directions for the Euclidean norm (left) and the max norm (right). In each panel, the dashed level set of $v \mapsto \langle -g, v \rangle$ supports the unit ball at $s_p(g)$.

The two cases in the figure are

$$s_2(g) = -\frac{g}{\|g\|_2}, \qquad s_\infty(g) = -\operatorname{sign}(g).$$

These formulas identify the directions followed by gradient descent and signed gradient descent, but not their step lengths. A second standard convention defines the *scaled steepest-descent vector*

$$d_p(g) \in \arg\min_v \left\{ \langle g, v\rangle + \frac{1}{2}\|v\|_p^2 \right\}. \tag{10.16}$$

For compatible choices of minimizers,

$$d_p(g) = \|g\|_q s_p(g), \qquad d_2(g) = -g, \qquad d_\infty(g) = -\|g\|_1 \operatorname{sign}(g).$$

Thus ordinary gradient descent is exactly scaled Euclidean steepest descent. Signed gradient descent is exactly unit max-norm steepest descent; signed descent follows the same direction as scaled max-norm steepest descent but uses a different step length.

The distinction between unit and scaled steepest descent determines which stepsize theorem applies. If

$$w_{t+1} = w_t + \alpha_t s_p(g_t) \quad \text{and} \quad w_{t+1} = w_t + \eta_t d_p(g_t),$$

then the updates agree precisely when

$$\alpha_t = \eta_t \|g_t\|_q. \tag{10.17}$$

For signed descent, the unit-direction lengths in Theorem 10.3.1 decrease to zero but have infinite sum. For ordinary gradient descent with a small constant multiplier, the actual unit-direction length is $\alpha_t = \eta\|g_t\|_2$ and shrinks with the gradient. General scaled steepest-descent results impose conditions on $\eta_t$; pure signed descent corresponds instead to the scaled multiplier $\eta_t/\|g_t\|_1$, which need not remain bounded. Hence agreement of directions is not enough to transfer a discrete-time theorem. Both parts of Theorem 10.3.1 fit the useful pattern that the actual movement tends to zero but has infinite cumulative length.

Let

$$\gamma_p^\star = \max_{\|u\|_p \le 1} \min_{i\in[n]} \langle u, z_i\rangle.$$

On separable data, $\gamma_p^\star > 0$. For continuous time, let

$$g(t) = \nabla L_n(w(t))$$

and consider the unit-speed steepest-descent flow

$$\dot{w}(t) = s_p(g(t)) = s_p\big(\nabla L_n(w(t))\big), \qquad w(0) = w_0. \tag{10.18}$$

Here $w : [0,\infty) \to \mathbb{R}^d$ is a function of time and $\dot{w}(t) = \frac{d}{dt}w(t)$; Eq. (10.18) is an ordinary differential equation relating the trajectory $w$ to its derivative. Thus $\|\dot{w}(t)\|_p = 1$. Positive rescaling of the right-hand side gives the same continuous trajectory with a different time parameterization.

**Theorem 10.4.1** (Steepest-descent flow maximizes the corresponding margin)**.** *For the flow in Eq. (10.18) on a linearly separable sample,*

$$\gamma_p(w(t)) \longrightarrow \gamma_p^\star.$$

*Every directional limit point $u$ satisfies $\min_i\langle u, z_i\rangle = \gamma_p^\star$ and $\|u\|_p = 1$; consequently, $u/\gamma_p^\star$ solves Eq. (10.13). If the maximum-margin direction is unique, then $w(t)/\|w(t)\|_p$ converges to that direction.*

*Proof.* Along the flow, write $w = w(t)$, $g = \nabla L_n(w)$, and $L = L_n(w)$, and suppress the dependence on $t$. A preliminary calculation, asked for in Exercise 3, gives

$$L \longrightarrow 0, \qquad \|w\|_p \longrightarrow \infty. \tag{10.19}$$

We prove the asymptotic comparison

$$-\frac{d}{dt}\log L \geq (\gamma_p^\star - \varepsilon)\frac{d}{dt}\|w\|_p \tag{10.20}$$

for every $\varepsilon \in (0, \gamma_p^\star)$ and all sufficiently large $t$.

Suppose first that Eq. (10.20) holds. Integrating the inequality from a sufficiently large fixed time $t_0$ to $T$ and using Eq. (10.19) gives

$$\liminf_{T\to\infty} \frac{-\log L_n(w(T))}{\|w(T)\|_p} \geq \gamma_p^\star - \varepsilon.$$

Exercise 4 asks you to write out this integration and the remaining finite-sum details. In particular, the finite sum defining $L_n$ and $L \to 0$ give

$$-\log L_n(w) = \min_{i\in[n]} \langle w, z_i\rangle + O(1).$$

After sending $\varepsilon \downarrow 0$ and using $\|w\|_p \to \infty$,

$$\liminf_{t\to\infty} \gamma_p(w(t)) \geq \gamma_p^\star.$$

The reverse inequality holds at every time by the definition of $\gamma_p^\star$. To finish the proof, it remains only to establish Eq. (10.20).

Choose $u_p^\star$ with $\|u_p^\star\|_p = 1$ and $\min_i \langle u_p^\star, z_i\rangle = \gamma_p^\star$. The flow definition and Eq. (10.15) give

$$-\dot{L} = -\langle g, \dot{w}\rangle = -\langle g, s_p(g)\rangle = \|g\|_q. \tag{10.21}$$

Moreover, letting $a_i = \frac{1}{n(1+e^{\langle w, z_i\rangle})}$, $i \in [n]$, we calculate

$$-g = -\nabla L_n(w) = \sum_{i=1}^n a_i z_i. \tag{10.22}$$

Consequently, norm duality and the definition of $u_p^\star$ give

$$\|g\|_q \geq \langle -g, u_p^\star\rangle = \sum_{i=1}^n a_i \langle z_i, u_p^\star\rangle \geq \gamma_p^\star A\,, \tag{10.23}$$

where we defined $A = \sum_i a_i$. Because $L \to 0$ and its finitely many summands are nonnegative, every margin tends to infinity. Hence $\frac{1}{1+e^m} \sim e^{-m}$ and $\log(1+e^{-m}) \sim e^{-m}$ imply $A/L \to 1$. Therefore, for all sufficiently large $t$,

$$-\frac{d}{dt}\log L = \frac{-\dot{L}}{L} = \frac{\|g\|_q}{L} \geq \gamma_p^\star \frac{A}{L} \geq \gamma_p^\star - \varepsilon. \tag{10.24}$$

Finally, the reverse triangle inequality gives, for $h > 0$,

$$\frac{\|w(t+h)\|_p - \|w(t)\|_p}{h} \leq \frac{\|w(t+h) - w(t)\|_p}{h}.$$

Letting $h \downarrow 0$ and using $\dot{w} = s_p(g)$ yields, for almost every $t$,

$$\frac{d}{dt}\|w\|_p \le \|\dot{w}\|_p = 1. \tag{10.25}$$

Combining Eqs. (10.24) and (10.25) proves Eq. (10.20). The margin conclusion follows from the first part of the argument. The statement about directional limit points follows from the equivalent norm-minimization formulation in Eq. (10.13). □

The theorem proves the continuous-time statement. The discrete result in Theorem 10.3.1 requires a separate one-step loss bound, and its assumptions depend on whether the update uses $s_p(g_t)$ or $d_p(g_t)$. Exercise 5 asks you to carry out this comparison for a scaled update and to translate between the two stepsize conventions using Eq. (10.17).

Ordinary gradient descent therefore constructs a Euclidean max-margin direction, while signed descent constructs a max-norm direction. Both fit the observed labels, but they can assign different signs to unobserved inputs. Population risk determines which extrapolation is useful. The next section makes this dependence exact.

## 10.5 A two-dimensional reversal

Optimization has now selected a direction. Does the selected direction affect population prediction? In an overparameterized problem, the training sample can constrain the score on observed inputs without determining the signs assigned to unseen inputs. The answer is therefore yes: two directions can classify the same training sample perfectly and have different population risks. We begin with the smallest exact example. The example also shows that either direction can be better, depending on the population law. Section 10.6 then turns the order-$1/n$ difference into a constant one.

Suppose the training sample contains only the signed vector

$$z_0 = (2, 1)^\top.$$

The hard-margin constraint is $\langle w, z_0\rangle \ge 1$.

**Proposition 10.5.1** (One observation produces two separators)**.** *For the constraint $\langle w, z_0\rangle \ge 1$, the minimum-$\ell_2$ and minimum-$\ell_\infty$ solutions are, respectively,*

$$w_2 = \left(\frac{2}{5}, \frac{1}{5}\right)^\top, \qquad w_\infty = \left(\frac{1}{3}, \frac{1}{3}\right)^\top.$$

*For*

$$u = (1, -3/2)^\top, \qquad v = (-1, 3/2)^\top,$$

*their signed scores have opposite signs:*

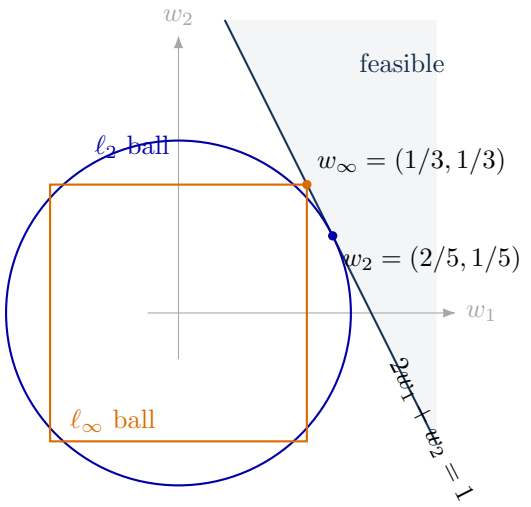
$$\langle w_2, u\rangle > 0 > \langle w_\infty, u\rangle, \qquad \langle w_\infty, v\rangle > 0 > \langle w_2, v\rangle.$$

*Proof.* The Euclidean solution is the projection of zero onto the constraint boundary, so $w_2 = z_0/\|z_0\|_2^2 = (2/5, 1/5)^\top$. Hölder's inequality gives $1 \le \langle w, z_0\rangle \le 3\|w\|_\infty$, with equality at $w_\infty = (1/3, 1/3)^\top$. Direct calculation gives

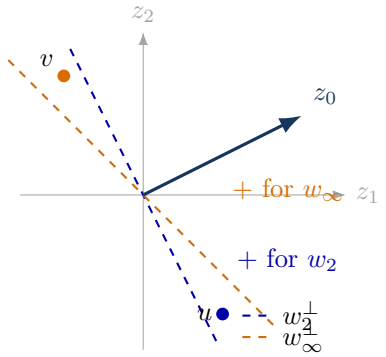
$$\langle w_2, u\rangle = \frac{1}{10}, \quad \langle w_\infty, u\rangle = -\frac{1}{6}, \quad \langle w_2, v\rangle = -\frac{1}{10}, \quad \langle w_\infty, v\rangle = \frac{1}{6}.$$

□

**(a) Selection in parameter space**




**(b) Scores in signed-feature space**




| Signed feature | $\operatorname{sign}\langle w_2, z\rangle$ | $\operatorname{sign}\langle w_\infty, z\rangle$ |
|---|---|---|
| $z_0 = (2, 1)$ | $+$ | $+$ |
| $u = (1, -3/2)$ | $+$ | $-$ |
| $v = (-1, 3/2)$ | $-$ | $+$ |

Figure 3: The same observed signed vector $z_0$ produces different Euclidean and max-norm separators. Panel (a) shows the two norm balls at their first contact with the hard-margin half-space. Panel (b) shows the resulting decision boundaries. A population with rare point $u$ favors Euclidean selection; replacing $u$ by $v$ favors max-norm selection.

The same example has a direct data-space interpretation. Regard $z_0$ as a positive example and $-z_0$ as a negative example. Both produce the signed feature $yx = z_0$, so both impose the same hard-margin constraint. Let $H_w = \{x : \langle w, x\rangle = 0\}$ and let $q$ be conjugate to $p$.

**Proposition 10.5.2** (Dual-norm distance to a hyperplane)**.** *Assume* $\langle w, z_0\rangle = 1$. *Then*

$$\operatorname{dist}_q(z_0, H_w) = \frac{\langle w, z_0\rangle}{\|w\|_p} = \frac{1}{\|w\|_p}.$$

*Proof.* For every $z \in H_w$, Hölder's inequality gives

$$1 = \langle w, z_0 - z\rangle \le \|w\|_p \|z_0 - z\|_q.$$

Hence $\operatorname{dist}_q(z_0, H_w) \ge 1/\|w\|_p$. By norm duality, there exists $s$ with $\|s\|_q = 1$ and $\langle w, s\rangle = \|w\|_p$. Setting

$$z = z_0 - \frac{s}{\|w\|_p}$$

gives $\langle w, z\rangle = 1 - 1 = 0$, so $z \in H_w$, and $\|z_0 - z\|_q = 1/\|w\|_p$. The matching upper bound proves equality. □

Thus minimizing the parameter norm $\|w\|_p$ maximizes the input-space margin measured in the dual norm $\|\cdot\|_q$.

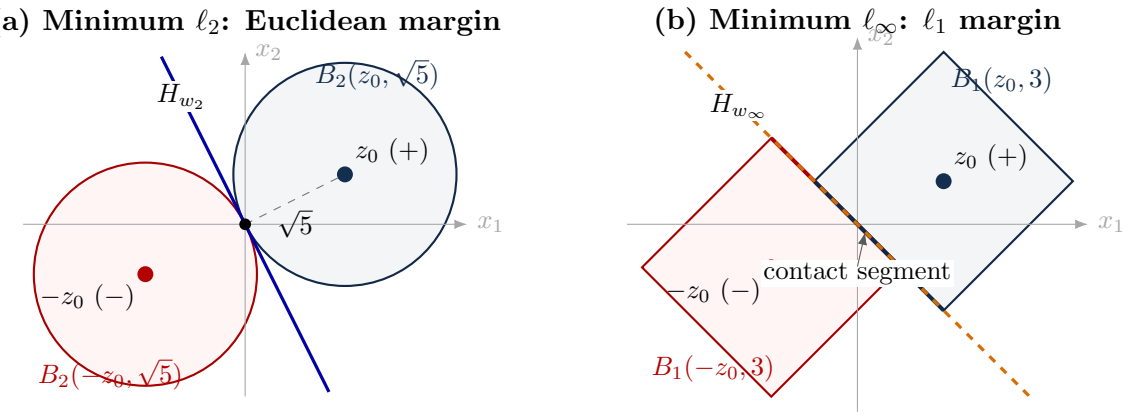



Figure 4: The two decision boundaries separate the positive point $z_0$ from the negative point $-z_0$. The Euclidean separator $H_{w_2}$ supports touching $\ell_2$ balls of radius $\sqrt{5}$. The max-norm separator $H_{w_\infty}$ supports $\ell_1$ balls of radius 3; because the $\ell_1$ ball is not strictly convex, contact occurs along line segments. The balls use the input-space norm dual to the norm minimized in parameter space.

We now make the generalization comparison exact. Let $Y$ be uniform on $\{-1, 1\}$ and independent of a signed feature $Z$, and set $X = YZ$. Then $YX = Z$. For $\delta \in (0, 1)$, define two population laws:

$$P_2: \quad \mathbb{P}(Z = z_0) = 1 - \delta, \qquad \mathbb{P}(Z = u) = \delta, \tag{10.26}$$

$$P_\infty: \quad \mathbb{P}(Z = z_0) = 1 - \delta, \qquad \mathbb{P}(Z = v) = \delta. \tag{10.27}$$

Both laws are linearly separable at the population level: $(1, 0)^\top$ separates the support of $P_2$, and $(0, 1)^\top$ separates the support of $P_\infty$.

For $p \in \{2, \infty\}$, let $\widehat{w}_p(S_n)$ be a minimum-$\ell_p$ solution of the empirical hard-margin constraints. For samples generated by these laws, the solution is unique except when both support points appear; when both points appear, any selected solution classifies both observed support points correctly.

**Theorem 10.5.3** (Either norm-induced selector can have smaller expected population risk)**.** *For every $n \geq 1$ and $\delta \in (0, 1)$,*

$$\mathbb{E}_{P_2^n}\left[R_{P_2}(\widehat{w}_\infty(S_n)) - R_{P_2}(\widehat{w}_2(S_n))\right] = \delta(1-\delta)^n,$$
$$\mathbb{E}_{P_\infty^n}\left[R_{P_\infty}(\widehat{w}_2(S_n)) - R_{P_\infty}(\widehat{w}_\infty(S_n))\right] = \delta(1-\delta)^n.$$

*The gap is maximized at $\delta = 1/(n+1)$ and is asymptotic to $1/(en)$.*

*Proof.* Let $E$ be the event that the common point $z_0$ is observed and the rare point is absent. The two selectors can disagree in population risk only on $E$, and $\mathbb{P}(E) = (1-\delta)^n$. Conditional on $E$, Proposition 10.5.1 shows that the disfavored selector misclassifies exactly the rare point, of population mass $\delta$. If both support points appear, both empirical constraints enforce correct classification of the entire support. If the sample contains only the rare point, the two selectors have the same population risk. These cases prove both identities.

For $g(\delta) = \delta(1-\delta)^n$,

$$g'(\delta) = (1-\delta)^{n-1}(1-(n+1)\delta),$$

so the unique maximizer is $\delta = 1/(n+1)$. At this value,

$$g(\delta) = \frac{1}{n+1}\left(\frac{n}{n+1}\right)^n \sim \frac{1}{en}.$$

□

This fixed two-dimensional construction makes the reversal transparent, but its largest expected gap vanishes with $n$. The next result shows why the effect can remain constant when the number of available features grows with the sample size.

## 10.6 A constant gap from private features

The two-dimensional example can be amplified without changing the global norm or splitting optimization into separate tasks. Each signed feature vector below has a two-dimensional shared block and an $n$-dimensional private block. Rare identity $j$ activates only coordinate $j$ of the private feature block. Training can therefore fit every observed identity by changing the corresponding private parameter coefficient. For an unobserved identity, that coefficient remains zero, so the shared block determines the prediction.

Fix the sample size $n \geq 4$ and set $d = n + 2$. Let $e_1, \ldots, e_n$ be the standard basis of $\mathbb{R}^n$, and write a signed feature as $(z^{\mathrm{sh}}, z^{\mathrm{pr}}) \in \mathbb{R}^2 \times \mathbb{R}^n$. The common signed feature vector is

$$z_0 = ((2,1)^\top, 0).$$

For each rare identity $j \in [n]$, define

$$u_j = ((1,-3/2)^\top, ne_j), \tag{10.28}$$

$$v_j = ((-1,3/2)^\top, ne_j). \tag{10.29}$$

The two coordinate blocks have different purposes. The shared vectors

$$u = (1,-3/2)^\top, \qquad v = (-1,3/2)^\top = -u$$

lie in the wedge between the two decision boundaries in Fig. 3: the Euclidean and max-norm selectors assign opposite signs to $u$, and their signs reverse at $v$. The first two coordinates therefore determine how a selector extrapolates to an unseen rare identity.

The basis vector $e_j$ specifies the private feature direction associated with identity $j$. If identity $j$ is observed, its margin can be repaired by changing only the corresponding private parameter coefficient. If identity $j$ is absent, minimum-norm selection leaves that coefficient at zero, and the prediction falls back to the shared two-dimensional score. The factor $n$ makes the repair cheap: a constant margin deficit requires a private coefficient of order $1/n$. Across at most $n$ observed identities, the total squared Euclidean cost is therefore only $O(1/n)$, and the absolute value of every private coefficient remains below the optimal max norm for large $n$. Geometrically, the construction consists of a common two-dimensional plane and one orthogonal private direction for each rare identity.

Under $P_{2,n}$, the signed feature $Z$ takes the value $z_0$ with probability $1/2$ and takes each value $u_j$ with probability $1/(2n)$. Under $P_{\infty,n}$, $u_j$ is replaced by $v_j$. As before, draw an independent uniform label $Y \in \{-1,1\}$ and set $X = YZ$. Both populations are linearly separable: the parameter with shared block $(1,0)^\top$ and zero private block separates $P_{2,n}$, while the parameter with shared block $(0,1)^\top$ and zero private block separates $P_{\infty,n}$.

Let $\widehat{w}_2$ be the minimum-$\ell_2$ empirical hard-margin separator. Let $\widehat{w}_\infty$ first minimize the global $\ell_\infty$ norm and then, among those solutions, minimize the Euclidean norm. The Euclidean tie-break only fixes otherwise irrelevant parameter coefficients. The tie-break agrees with zero initialization on the coefficients associated with identities absent from the sample.[1]

The event that at least one common example appears will be denoted by

$$G_n = \{z_0 \text{ occurs in } S_n\}.$$

The complement $G_n^c$ has probability $2^{-n}$.

**Lemma 10.6.1** (The shared parameter blocks retain the two-dimensional biases)**.** *On $G_n$, the shared coordinates of $\widehat{w}_\infty$ equal $(1/3, 1/3)^\top$. The shared coordinates $\widehat{w}_2^{\mathrm{sh}}$ satisfy*

$$\left\| \widehat{w}_2^{\mathrm{sh}} - \left(\frac{2}{5}, \frac{1}{5}\right)^\top \right\|_2^2 \le \frac{121}{100n}.$$

*Every private parameter coefficient associated with an identity absent from $S_n$ is zero for both selectors.*

*Proof.* The common constraint is $2w_1 + w_2 \ge 1$. Hence $\|w\|_\infty \ge 1/3$, with equality only if $w_1 = w_2 = 1/3$. For an observed $u_j$, the shared score of $u_j$ is $-1/6$, and setting the corresponding private parameter coefficient to $7/(6n)$ raises the margin to one. For an observed $v_j$, the required coefficient is $5/(6n)$. These values are at most $1/3$ for $n \ge 4$, so a feasible separator with max norm $1/3$ exists. The shared coordinates of every max-norm minimizer are therefore exactly $(1/3, 1/3)^\top$. The Euclidean tie-break sets every unused private parameter coefficient to zero.

For the Euclidean problem, write $w_2^\star = (2/5, 1/5)^\top$. A feasible comparison vector uses shared coordinates $w_2^\star$ and, for every observed rare identity, a private parameter coefficient $9/(10n)$ under $P_{2,n}$ or $11/(10n)$ under $P_{\infty,n}$. There are at most $n$ observed identities, so the squared norm of the comparison vector is at most

$$\|w_2^\star\|_2^2 + n\left(\frac{11}{10n}\right)^2 = \frac{1}{5} + \frac{121}{100n}.$$

The common constraint and $w_2^\star = z_0^{\mathrm{sh}}/5$ imply, for every feasible shared vector $a$,

$$\|a\|_2^2 = \|w_2^\star\|_2^2 + 2\langle w_2^\star, a - w_2^\star\rangle + \|a - w_2^\star\|_2^2 \ge \frac{1}{5} + \|a - w_2^\star\|_2^2.$$

The Euclidean minimizer has no larger norm than the comparison vector; combining this comparison with the preceding inequality proves the bound. Finally, an unused private parameter coefficient appears in no constraint, so setting that coefficient to zero strictly decreases either Euclidean norm used in the two selection rules unless the coefficient was already zero. □

The Euclidean bound tends to zero. Since the shared Euclidean margins on $(1, -3/2)^\top$ and $(-1, 3/2)^\top$ are $1/10$ and $-1/10$, respectively, the signs of these margins agree with the original two-dimensional example for all sufficiently large $n$.

**Theorem 10.6.2** (Global norm selection can differ by a constant in either direction)**.** *For the minimum-$\ell_2$ and minimum-$\ell_\infty$ selectors above,*

$$\mathbb{E}_{P_{2,n}^n}[R_{P_{2,n}}(\widehat{w}_2)] \longrightarrow 0, \qquad \mathbb{E}_{P_{2,n}^n}[R_{P_{2,n}}(\widehat{w}_\infty)] \longrightarrow \frac{1}{2}e^{-1/2},$$

$$\mathbb{E}_{P_{\infty,n}^n}[R_{P_{\infty,n}}(\widehat{w}_\infty)] \longrightarrow 0, \qquad \mathbb{E}_{P_{\infty,n}^n}[R_{P_{\infty,n}}(\widehat{w}_2)] \longrightarrow \frac{1}{2}e^{-1/2}.$$

*Thus the limiting gap in either direction is approximately* 0.303*.*

*Proof.* On $G_n$, every observed rare identity is classified correctly because the corresponding hard-margin constraint is present. For an unobserved rare identity, the associated private parameter coefficient is zero by Lemma 10.6.1. Under $P_{2,n}$, the Euclidean shared score on every $u_j$ is positive for all sufficiently large $n$, while the max-norm shared score is $-1/6$. Under $P_{\infty,n}$, the max-norm shared score on every $v_j$ is $1/6$, while the Euclidean shared score is negative for all sufficiently large $n$. The favored selector under each population law therefore has zero risk on $G_n$, and its expected risk is at most $\mathbb{P}(G_n^c) = 2^{-n}$.

For a fixed rare identity $j$, the probability that it is absent while a common point is present is

$$\left(1 - \frac{1}{2n}\right)^n - \left(\frac{1}{2} - \frac{1}{2n}\right)^n.$$

Each rare signed-feature value has population mass $1/(2n)$. Summing over the $n$ rare signed-feature values, the disfavored selector's expected error on $G_n$ is

$$\frac{1}{2}\left[\left(1 - \frac{1}{2n}\right)^n - \left(\frac{1}{2} - \frac{1}{2n}\right)^n\right] \longrightarrow \frac{1}{2}e^{-1/2}. \tag{10.30}$$

The contribution of $G_n^c$ is at most $2^{-n}$, proving all four limits. □

Here $d = n + 2$, so the construction is in the proportional-dimensional, slightly overparameterized regime. The construction is a sequence of problems whose dimension and feature magnitudes grow with $n$. The theorem does not establish inconsistency for one fixed finite-dimensional distribution.[2]

The statistical mechanism is close to the example of Wilson et al. [2017]. There are recurring features that determine performance on new examples and private features that permit the classifier to fit the training sample but do not transfer to an unseen identity. The selected geometry determines how much the fitted classifier relies on each kind of feature.

## 10.7 Adam can move from max-norm to Euclidean bias

For a gradient $g_t = \nabla L_n(w_t)$, bias-corrected Adam forms coordinatewise exponential averages $\widehat{m}_t$ and $\widehat{v}_t$ of $g_t$ and $g_t^2$, then updates

$$w_{t+1} = w_t - \eta_t \frac{\widehat{m}_t}{\sqrt{\widehat{v}_t} + \epsilon}. \tag{10.31}$$

All operations in the fraction are coordinatewise. The positive stability constant $\epsilon$ prevents division by zero.

When $\sqrt{\widehat{v}_t}$ dominates $\epsilon$ and the moving averages track a nearly constant gradient direction, the denominator approximately normalizes each coordinate and the update is sign-like. When the gradients have become small relative to $\epsilon$, the denominator is approximately constant and the update is gradient-like. These two limiting calculations suggest two geometries, but the calculations do not by themselves determine which parameter direction the entire trajectory approaches.

The following statement summarizes a recent result for deterministic, full-batch, bias-corrected Adam on separable linear logistic classification. The result uses polynomially decreasing stepsizes and fixed $\epsilon > 0$, together with regularity conditions ensuring the standard max-margin limits. The comparison is made as $\epsilon \downarrow 0$.

**Theorem 10.7.1** (Adam has early max-norm and late Euclidean regimes)**.** *For sufficiently small fixed $\epsilon > 0$, Adam reaches parameter vectors with nearly optimal $\ell_\infty$ normalized margin before its updates become gradient-like. At much later times its normalized parameter vector approaches the minimum-$\ell_2$ hard-margin direction.*

*Proof outline.* When $\sqrt{\widehat{v}_t} \gg \epsilon$ coordinatewise, division by $\sqrt{\widehat{v}_t}$ normalizes the gradient magnitudes. After controlling the errors caused by the moving averages, the resulting update direction is a perturbation of the signed-descent direction and inherits its $\ell_\infty$ max-margin behavior. The perturbation argument establishes a time interval on which the normalized margin is arbitrarily close to the optimal $\ell_\infty$ margin as $\epsilon \downarrow 0$.

Because the data are separable, the logistic gradients vanish along the trajectory. For every fixed $\epsilon > 0$, eventually $\sqrt{\widehat{v}_t} \ll \epsilon$. The denominator in Eq. (10.31) is then $\epsilon(1 + o(1))$, and the first-moment average tracks the ordinary gradient closely enough that Adam is an asymptotically vanishing perturbation of Euclidean gradient descent. The Euclidean part of Theorem 10.3.1 then gives the late minimum-$\ell_2$ direction. The complete argument proves that the max-norm interval occurs before the Euclidean asymptotic regime by bounding the two timescales uniformly in small $\epsilon$. □

The point for this lecture is the distinction between the two selected directions, not the detailed crossover. The normalized parameter vector can remain close to the max-norm direction after the update has already become gradient-like; the earlier updates have built a large component that later updates must replace.[3]

**Corollary 10.7.2** (The preferred checkpoint depends on the population law)**.** *In the two laws of Theorem 10.5.3, a checkpoint whose parameter direction is sufficiently close to the max-norm separator is preferred under $P_\infty$, while a checkpoint sufficiently close to the Euclidean separator is preferred under $P_2$.*

*Proof.* For each sample-support pattern in the two-point construction, the relevant Euclidean and max-norm separators assign nonzero scores to both population support points. Classification risk is therefore constant in a sufficiently small neighborhood of each separator. Apply Theorem 10.7.1 to choose an early checkpoint in the max-norm neighborhood and a late checkpoint in the Euclidean neighborhood. The expected-risk identities in Theorem 10.5.3 then give the two stated preferences. □

The corollary conditionally transfers the two-selector calculation; the corollary is not an exact finite-time risk formula for Adam. The conclusion is that stopping later can improve or worsen population classification even after the training sample has become perfectly classified. The sign of the change depends on the population law.

The practical response is to retain checkpoints and select among them using held-out data. Validation does not identify a universally correct optimizer; validation tests which point on the realized trajectory predicts better for the available validation distribution.

There is no conflict with the construction of Wilson et al. [2017]. Their published exact example concerns least-squares classification and idealized adaptive methods whose denominator has no fixed positive stability constant. With $\epsilon = 0$, coordinate normalization can persist forever. With fixed $\epsilon > 0$, the denominator eventually stops normalizing vanishing gradients, which permits the late Euclidean regime in separable logistic classification. In least squares, moreover, an early adaptive update can create a null-space component. Later ordinary gradients lie in the data row space and cannot remove that component.

## 10.8 Stepsize schedules determine whether noise persists

The word "stochastic" does not by itself determine the long-run behavior of an optimization method. The stepsize schedule determines whether successive perturbations become negligible or continue to

accumulate. The following one-dimensional calculation gives the basic distinction exactly.

Fix $\mu > 0$ and consider the quadratic objective $L(\theta) = \mu\theta^2/2$. Let $\Xi_1, \Xi_2, \dots$ be independent random variables with mean zero and variance $\sigma^2 > 0$. Starting from a fixed $\theta_0$, use the unbiased stochastic gradient $\mu\Theta_t + \Xi_{t+1}$:

$$\Theta_{t+1} = \Theta_t - \eta_t(\mu\Theta_t + \Xi_{t+1}). \tag{10.32}$$

**Proposition 10.8.1** (Constant-stepsize iterates fluctuate; decreasing-stepsize iterates converge)**.** *For the recursion in Eq. (10.32):*

*(a) If $\eta_t = \eta \in (0, 2/\mu)$, then*

$$\mathbb{E}[\Theta_t] \longrightarrow 0, \qquad \mathrm{Var}(\Theta_t) \longrightarrow \frac{\eta\sigma^2}{\mu(2-\mu\eta)} > 0.$$

*(b) If $\eta_t = 1/(\mu(t+1))$, then, for every $t \geq 1$,*

$$\Theta_t = -\frac{1}{\mu t}\sum_{s=1}^{t}\Xi_s, \qquad \mathbb{E}[\Theta_t^2] = \frac{\sigma^2}{\mu^2 t}.$$

*Consequently, $\Theta_t \to 0$ in mean square and almost surely.*

*Proof.* For a constant stepsize, set $a = 1 - \mu\eta$, so $|a| < 1$. Independence and zero mean give

$$\mathbb{E}[\Theta_{t+1}] = a\mathbb{E}[\Theta_t], \qquad \mathrm{Var}(\Theta_{t+1}) = a^2\,\mathrm{Var}(\Theta_t) + \eta^2\sigma^2.$$

The variance recursion converges to $\eta^2\sigma^2/(1-a^2) = \eta\sigma^2/[\mu(2-\mu\eta)]$. For the decreasing schedule, induction in Eq. (10.32) gives the displayed empirical average. Its second moment is $\sigma^2/(\mu^2 t)$, and almost-sure convergence follows from the strong law of large numbers. □

Under a constant stepsize, the distribution of the iterate retains nonzero spread around the unique minimizer; the iterate does not approach the minimizer itself. The limiting standard deviation is of order $\sqrt{\eta}$. A smaller constant stepsize reduces this spread but does not remove the asymptotic fluctuation. The decreasing schedule eventually suppresses the noise.

The general stochastic-approximation conditions

$$\sum_{t=0}^{\infty}\eta_t = \infty, \qquad \sum_{t=0}^{\infty}\eta_t^2 < \infty \tag{10.33}$$

express the same balance. The first sum leaves enough cumulative movement to reach a solution; the second makes the cumulative variance of bounded mean-zero perturbations finite. Additional assumptions are needed for a general convergence theorem, especially for a nonconvex objective.

Constant stepsize has a different effect when the set of minimizers contains a curve or manifold with tangent directions along which there is no restoring gradient. After $t$ independent mean-zero increments of size $\eta$, the accumulated displacement has standard deviation of order $\eta\sqrt{t}$. The resulting variance accumulation is *diffusive behavior*: order-one motion along a flat solution set occurs on the timescale $t \asymp \eta^{-2}$. State-dependent noise can also create a systematic drift along the flat solution set and thereby prefer some solutions to others. At an isolated unique minimizer, the same noise instead produces a stationary distribution concentrated near that point.

There is an important exception. Constant stepsize does not create persistent motion when the stochastic gradient noise itself vanishes at every exact fit. For squared-loss prediction, let

$$\ell_i(\theta) = \frac{1}{2}\big(f_\theta(x_i) - y_i\big)^2.$$

**Proposition 10.8.2** (Interpolation can remove minibatch noise)**.** *If $f_\theta(x_i) = y_i$ for every training example, then every per-example and minibatch gradient is zero at $\theta$.*

*Proof.* For every $i$,

$$\nabla \ell_i(\theta) = \big(f_\theta(x_i) - y_i\big)\nabla f_\theta(x_i) = 0.$$

Every minibatch gradient is an average of these vectors. □

This proposition explains why minibatch SGD and gradient descent have the same minimum-norm bias in interpolating linear least squares. In a nonconvex network, minibatch noise may still change the basin reached before interpolation, but the minibatch noise stops once every individual residual is zero. Continued motion along a zero-loss set requires nonvanishing noise, such as fresh label perturbations, or another mechanism that prevents every individual gradient from vanishing.

The disappearance of minibatch noise differs from a common stochastic-approximation model in engineering, in which every gradient query contains fresh measurement or simulation noise whose variance remains positive at a minimizer. Minibatch noise from a fixed finite empirical objective is state dependent. Whether noise persists at a solution is therefore a property of the loss, data, and noise mechanism, not an automatic consequence of using a stochastic update.

Practical schedules often use long constant-stepsize phases followed by one or more reductions. During a constant phase, persistent noise can explore or move along a set of low-loss parameters. Reducing the stepsize concentrates the iterates and can eventually fix one of those parameters. A stepsize reduction can change population performance only when the points visited by the dynamics define different predictors or extrapolate differently; stochasticity alone gives no ordering of their population risks.

## 10.9 What the examples establish

Does the direction selected by the optimizer matter? Yes, when the empirical constraints leave predictions on unobserved inputs undetermined. The two-dimensional example gives an exact order-$1/n$ effect, and the proportional-dimensional example gives a constant effect. Neither direction is universally better. The examples and the noisy-quadratic calculation support four specific conclusions.

First, the empirical objective need not determine the returned predictor. In least squares, initialization fixes the component orthogonal to the data span. In separable logistic classification, the update geometry fixes a limiting margin geometry.

Second, an optimizer-induced preference is not automatically a statistically correct preference. Euclidean and max-norm selection each win on one of the two population laws. A norm can be useful only relative to structure in the data-generating law, such as which features or contexts recur at test time.

Third, growing dimension can change the magnitude of the effect. The two-dimensional ambiguity occurs only when one rare point is missing, giving an order-$1/n$ maximal expected gap. With $\Theta(n)$ rare identities, a constant fraction of population mass can belong to identities absent from the sample, giving a constant gap.

Fourth, the stepsize schedule determines the asymptotic role of gradient noise. Decreasing stepsizes can permit convergence by making the cumulative noise variance finite. A constant stepsize with persistent noise produces a stationary fluctuation near an isolated solution or diffusive motion along a solution set. If every stochastic gradient vanishes at interpolation, even a constant stepsize supplies no continuing noise.

The linear setting isolates optimizer-induced selection exactly. The linear analysis does not describe feature learning in a deep network and does not imply that Adam or SGD is uniformly preferable in applications. Empirical comparisons have found both meaningful optimizer-dependent gaps and substantial dependence on tuning, architecture, and task. The theorem-level conclusion is the absence of a universal ordering.

## 10.10 Optional reading*

### 10.10.1 Early stopping induces a spectral filter

Return to least squares with $w_0 = 0$. Set $H = \mathbf{X}^\top \mathbf{X}$ and $b = \mathbf{X}^\top y$. Suppose $0 < \eta < 2/\|H\|_{\mathrm{op}}$, and write

$$H = \sum_{j=1}^{d} \lambda_j q_j q_j^\top$$

for an orthonormal eigenbasis, with $\lambda_j \geq 0$.

**Proposition 10.10.1** (Finite-time gradient descent filters eigendirections)**.** *For every $t \geq 1$,*

$$w_t = \sum_{j:\lambda_j > 0} \frac{1 - (1 - \eta\lambda_j)^t}{\lambda_j} \langle q_j, b \rangle q_j.$$

*Proof.* The update is $w_{t+1} = (I - \eta H) w_t + \eta b$. Since $w_0 = 0$, unrolling the recurrence gives

$$w_t = \eta \sum_{k=0}^{t-1} (I - \eta H)^k b.$$

Moreover, $b = \mathbf{X}^\top y$ is orthogonal to $\ker H$. Along the eigendirection spanned by $q_j$ with $\lambda_j > 0$, the coefficient is therefore

$$\eta \sum_{k=0}^{t-1} (1 - \eta\lambda_j)^k \langle q_j, b \rangle = \frac{1 - (1 - \eta\lambda_j)^t}{\lambda_j} \langle q_j, b \rangle.$$

Summing these coefficients proves the formula. □

The scalar function

$$g_t(\lambda) = \frac{1 - (1 - \eta\lambda)^t}{\lambda}$$

is a *spectral filter*: the function $g_t$ specifies how strongly the procedure responds to the data in each eigendirection of $H$. At convergence, $g_\infty(\lambda) = 1/\lambda$. At finite time, if $\eta t \lambda \ll 1$, then $g_t(\lambda) \approx \eta t$. Thus early stopping does not yet apply the large inverse factor $1/\lambda$ to directions with small eigenvalues. The transition occurs around $\lambda \approx 1/(\eta t)$. Ridge regression uses the related filter $g_\rho(\lambda) = 1/(\lambda + \rho)$.

The filter formula explains why a stopping time can act as regularization even before considering different limiting optima: the stopping time changes which spectral components have had time to enter the solution. Exercise 9 asks you to derive the formula and compare the two filters.

### 10.10.2 The Wilson construction

The least-squares construction of Wilson et al. [2017] uses one feature coordinate that reveals the label, two constant feature coordinates, and many feature coordinates that are nonzero in only one training example. Zero-initialized gradient methods remain in the row span and reach the minimum-$\ell_2$ interpolant. In their example, the minimum-$\ell_2$ classifier uses the recurring label feature and has asymptotically zero classification error. AdaGrad, RMSProp, and Adam without a positive stability offset follow a coordinate-normalized ray that assigns the same parameter-coordinate magnitude to private and recurring features; the resulting classifier predicts the majority class on new examples and can have error arbitrarily close to $1/2$. A finite version uses $O(n)$ features.

Their exact ray calculation is not specific to squared loss. Let $\mathbf{X}$ have row $i$ equal to $x_i^\top$, let $y \in \{-1, 1\}^n$, set $s = \operatorname{sign}(\mathbf{X}^\top y)$, and suppose

$$\mathbf{X}s = cy \tag{10.34}$$

for some $c > 0$.

**Proposition 10.10.2** (Equal margins preserve the signed-gradient ray)**.** *For any differentiable margin loss $L(w) = \sum_{i=1}^n \ell(y_i \langle w, x_i \rangle)$ and every $\alpha \geq 0$,*

$$\nabla L(\alpha s) = \ell'(c\alpha)\mathbf{X}^\top y.$$

*If $\ell' < 0$, signed gradient descent initialized at zero remains on the ray $\{\alpha s : \alpha \geq 0\}$.*

*Proof.* Equation Eq. (10.34) gives $y_i \langle s, x_i \rangle = c$ for every $i$. Hence

$$\nabla L(\alpha s) = \sum_{i=1}^n \ell'(c\alpha) y_i x_i = \ell'(c\alpha)\mathbf{X}^\top y.$$

Since $s = \operatorname{sign}(\mathbf{X}^\top y)$ and $\ell' < 0$, the negative signed gradient is $s$ on every nonzero coordinate. Induction proves the ray claim. □

Logistic loss satisfies the proposition, so the equal-margin ray remains invariant for logistic loss when the adaptive denominator exactly cancels coordinate magnitudes. The proposition does not extend the published population theorem to ordinary Adam with fixed $\epsilon > 0$: the added $\epsilon$ breaks exact coordinate cancellation as gradients vanish. Exercise 8 asks you to verify both the margin-loss and squared-loss calculations.

### 10.10.3 Noisy selection in neural networks and flatness

Proposition 10.8.2 shows that ordinary minibatch noise vanishes at squared-loss interpolation. A clean way to keep stochasticity active is to perturb the label afresh at every update. Consider

$$L(\theta) = \frac{1}{2n} \sum_{i=1}^n \big(f_\theta(x_i) - y_i\big)^2$$

and its zero-training-error set

$$\mathcal{M} = \{\theta : f_\theta(x_i) = y_i \text{ for every } i\}.$$

At an update using example $i$, replace $y_i$ by $y_i + \Xi$, where $\Xi$ has mean zero and variance $\sigma^2$ and is sampled independently at each step. At $\theta \in \mathcal{M}$, the gradient contribution is $-\Xi \nabla f_\theta(x_i)$, so its covariance depends on the network Jacobians. The corresponding scalar quantity is

$$\mathcal{R}(\theta) = \frac{1}{n} \sum_{i=1}^{n} \|\nabla f_\theta(x_i)\|_2^2 = \operatorname{tr}\big(\nabla^2 L(\theta)\big), \qquad \theta \in \mathcal{M}. \tag{10.35}$$

The equality uses the zero residuals: the residual-weighted second-derivative terms in the Hessian vanish on $\mathcal{M}$.

The next statement summarizes a local small-stepsize result for smooth networks with bounded derivatives and independent bounded label noise of constant variance. The setup is deliberately different from ordinary minibatch SGD on an exactly interpolated dataset.

**Theorem 10.10.3** (Label-noise dynamics select minimizers of a Jacobian regularizer)**.** *A zero-training-error parameter is locally attractive for the label-noise training dynamics precisely when it is a local minimizer of $\mathcal{R}$ restricted to the zero-error manifold $\mathcal{M}$.*

*Proof outline.* Near $\mathcal{M}$, decompose a parameter displacement into components normal and tangent to the manifold. The squared-loss Hessian contracts the normal component. Fresh label perturbations keep producing normal fluctuations, so for a small constant stepsize this fast component approaches a local Ornstein–Uhlenbeck-type equilibrium rather than vanishing.

A second-order expansion of the update, averaged over these fast fluctuations, produces a slower tangential drift. Its leading term is a vector proportional to

$$-P_{T_\theta \mathcal{M}} \nabla \mathcal{R}(\theta),$$

where $P_{T_\theta \mathcal{M}}$ is the orthogonal projection operator onto the tangent space of $\mathcal{M}$. Thus the averaged slow dynamics descend the restriction of $\mathcal{R}$ to $\mathcal{M}$. Under the stated smoothness and boundedness assumptions, the higher-order terms are uniformly smaller for a sufficiently small stepsize. The locally attractive zero-error parameters are therefore exactly the constrained local minima of $\mathcal{R}$. The cited paper gives the perturbation bounds that justify the fast–slow averaging. □

The theorem is a genuine optimizer-induced selection result for neural networks of arbitrary smooth architecture. The label-noise dynamics have two timescales: the loss first becomes small, and the persistent noise then produces much slower motion within $\mathcal{M}$. A more general diffusion analysis describes the slow motion by a stochastic differential equation on the solution manifold. Both the drift and the covariance of this stochastic differential equation depend on the loss and on the covariance of the injected noise. Isotropic noise, label noise, and minibatch noise therefore need not select the same parameters.

The theorem does not say that minimizing $\mathcal{R}$ always improves population risk. An improvement in population risk requires an additional argument connecting the Jacobian regularizer to the data-generating law. Such a connection has been proved in some simplified nonlinear models, but not for arbitrary deep networks.

The label-noise result also gives a precise sense in which noise can prefer "flatter" parameters, but the result does not validate an unspecified flat-minimum principle. For a ReLU unit,

$$a\,[b^\top x]_+ = \frac{a}{c}\,[(cb)^\top x]_+, \qquad c > 0. \tag{10.36}$$

The two parameter vectors define the same predictor, but raw Hessian eigenvalues and parameter-space neighborhood volumes can change under the rescaling. Consequently, parameter-space

sharpness is not by itself a function of the learned predictor and cannot by itself explain a difference in population risk. The parameterization dependence does not rule out every invariant or algorithm-relative notion of flatness. The rescaling example rules out treating an arbitrary raw Hessian measure as a parameterization-independent explanation. In Theorem 10.10.3, the parameterization-dependent quantity is meaningful because $\mathcal{R}$ is derived from a specified update rule and noise model.

## 10.11 Take-home messages

- A decreasing stepsize can suppress stochastic-gradient noise and permit convergence. A constant stepsize with persistent noise instead produces a stationary fluctuation near an isolated minimizer or diffusive motion along a solution set. Constant stepsize alone is insufficient: at squared-loss interpolation, ordinary minibatch noise vanishes.
- The empirical objective may leave the predictor underdetermined. Initialization and update geometry then complete the selection rule: zero-initialized least-squares gradient descent selects the minimum-$\ell_2$ interpolant, while different steepest-descent geometries select different max-margin directions.
- Minimum-$\ell_2$ and minimum-$\ell_\infty$ selection can have opposite population-risk orderings. The data-generating law, not the empirical fit alone, determines which extrapolation is useful.
- A fixed two-dimensional problem gives an order-$1/n$ expected gap. With $\Theta(n)$ private features, the gap can approach $e^{-1/2}/2 \approx 0.303$. Adam can move from the max-norm geometry toward the Euclidean geometry, so an early or late checkpoint can be preferable depending on the population.

## Endnotes

1. The minimum-$\ell_\infty$ problem can have multiple solutions. The conclusions use only two properties of the tie-break: a private parameter coefficient associated with an unobserved identity remains zero, and no parameter coordinate exceeds the optimal max norm. Zero-initialized coordinatewise methods have the first property because no observed gradient has a component in that coordinate direction.

2. The nonzero entry in each private feature block has magnitude $n$ so that fitting all observed private identities changes the shared block of the minimum-Euclidean-norm separator by only $O(n^{-1/2})$. The growing scale is part of this exact construction and should not be hidden.

3. For stepsizes $\eta_t \asymp (t+1)^{-a}$ with $1/3 < a < 1$, the submitted analysis places the update crossover at a polylogarithmic scale in $1/\epsilon$, while reaching a fixed Euclidean-margin accuracy requires a polynomial scale in $1/\epsilon$. For $a = 1$, the corresponding separation is polynomial versus exponential. These rates are not needed for the risk examples in this lecture.

## Bibliographical notes

The Euclidean max-margin limit of discrete gradient descent on separable logistic regression is due to Soudry et al. [2018]. The treatment of implicit bias in terms of mirror-descent and steepest-descent geometry, including general norms, follows Gunasekar et al. [2018]. The discrete normalized steepest-descent and signed-gradient result stated in Theorem 10.3.1 follows the analysis of Fan et al. [2025]; its decreasing-stepsize assumptions should not be replaced by a generic appeal to the continuous-time limit. Balles and Hennig [2018] explain the relation between sign-based updates and steepest descent in max norm.

The examples in Sections 10.5 and 10.6 were developed for these notes to make the population-risk reversal explicit in both directions. The private-feature construction is inspired by the use of many example-specific features in Wilson et al. [2017]; no priority claim is made for the construction. Wilson et al. give a squared-loss example in which standard gradient methods generalize well and AdaGrad, RMSProp, and Adam can approach chance error. They also report optimizer-dependent differences on CIFAR-10 and language tasks. Later benchmark studies, including Sivaprasad et al. [2020], emphasize that such comparisons depend strongly on tuning and experimental protocol.

The separability and steepest-direction diagrams were typeset by Diego Gomez from the pictures used in class.

The two-regime Adam statement summarizes Fan and Szepesvári [2026]. Its endpoint results build on Wang et al. [2022]; Zhang et al. [2024a]: zero-offset Adam has max-norm margin bias, whereas fixed-positive-offset Adam eventually has Euclidean margin bias. Related work studies how optimizer geometry interacts with modern architectures and feature structure; examples include Schmidt et al. [2021]; Zhang et al. [2024b] and Vasudeva et al. [2025].

The stepsize calculation in Proposition 10.8.1 is an elementary instance of classical stochastic approximation. The local stationary-distribution view of constant-stepsize SGD is developed by Mandt et al. [2017]. The label-noise characterization in Theorem 10.10.3 is due to Blanc et al. [2020]; Li et al. [2022] give a general diffusion framework for motion near a smooth manifold of minimizers. Complete statistical comparisons are known in simpler nonlinear parameterizations. For example, HaoChen et al. [2021] show that the noise covariance changes sparse recovery in a quadratically parameterized model, and Pesme et al. [2021] compare stochastic and deterministic

gradient flows in diagonal linear networks. These results support a noise-model-dependent selection principle, not a universal advantage for SGD.

The spectral-filter view of iterative regularization is classical; see Yao et al. [2007]. The caution about parameter-space sharpness and the ReLU rescaling example follow Dinh et al. [2017]. Flatness can still enter valid generalization analyses after the relevant parameterization, perturbation, or invariant quantity is specified; the objection is to an unqualified raw Hessian explanation.

## Glossary

**Algorithmic bias**
In this lecture, the preference among empirical solutions or limiting directions induced by an optimization algorithm. We use the term only in this optimization sense.

**Explicit regularization**
Adding or imposing an auxiliary criterion that prefers some empirical solutions, such as a norm penalty or constraint.

**Diffusive behavior**
Accumulation of persistent mean-zero perturbations whose variance grows proportionally to time in directions without a restoring gradient.

**Gradient noise**
The difference between a stochastic gradient and the corresponding full empirical gradient. Its magnitude and covariance can depend on the current parameter.

**Implicit bias**
The preference among empirical solutions or limiting directions induced by the initialization, update geometry, or stopping rule while the empirical objective is fixed.

**Logit**
A real-valued score interpreted as log-odds. In binary logistic regression, $\langle w, x\rangle = \log(q_w(1 \mid x)/q_w(-1 \mid x))$.

**Linearly separable sample**
A labeled sample for which one linear score has strictly positive signed margin on every observed example.

**Margin**
The signed score $y\langle w, x\rangle$; after normalization by a norm of $w$, the resulting normalized margin is invariant to positive rescaling of the parameter vector $w$.

**Margin loss**
A training loss $\ell(ys(x))$ that depends on a labeled example through its signed margin.

**Model non-uniqueness**
The existence of empirically optimal parameters that represent different predictors on at least one input.

**Normalized empirical margin**
The smallest signed score on the training sample divided by a specified norm of the parameter. The normalized empirical margin depends only on the direction of a nonzero parameter vector.

**Max-margin separator**
A parameter direction that separates the sample and maximizes the smallest normalized empirical margin. Equivalently, it is the direction of a minimum-norm vector satisfying unit hard-margin constraints.

**Overparameterized**
A regime in which the parameterization has more degrees of freedom than the observed constraints need, so many exact empirical fits can exist.

**Parameter-space non-uniqueness**
The existence of distinct empirically optimal parameter vectors, possibly representing the same predictor.

**Strictly proper scoring rule**
A probability-prediction loss whose conditional expected value is uniquely minimized by reporting the true conditional distribution.

**Regularizer**
An auxiliary parameter- or predictor-dependent criterion used to prefer some fits to others.

**Spectral filter**
A scalar response function that specifies how a linear estimator weights each eigendirection of a data-dependent matrix.

**Steepest descent**
An optimization method that chooses the direction of greatest local decrease measured in a specified norm. Changing the norm changes the update geometry.

**Surrogate loss**
A tractable training loss used in place of the deployment loss that directly defines the task evaluation.

## 10.12 Exercises

**General instructions.** Justify every answer, including yes/no answers, even when the question does not explicitly ask for a justification.

**Exercise profiles.** Filled mountains show difficulty on a four-mountain scale: one is a direct application, two uses a familiar method, three combines ideas, and four is a substantial challenge. Filled cogs show technical load on a three-cog scale: one is light, two is sustained, and three is dense. Filled hourglasses show estimated time: one is under 20 minutes, two is 20–45 minutes, three is 45–90 minutes, and four is more than 90 minutes. Pale pictograms show the unused part of each scale. The work row uses the canonical order proof, calculation, construction, computation, and interpretation; pale icons mark work types not used. marks the intended learning outcome. Time estimates cover the non-optional parts. Ratings are not prerequisites or grading weights. A superscript asterisk marks an exercise based on supplementary lecture material; it is not a difficulty rating and does not make the exercise optional when assigned.



**Exercise 1: Initialization and the minimum-norm least-squares solution.**

◎ Identify the invariant component of least-squares gradient descent and derive the solution selected by its initialization.

Fix $x_1, \dots, x_n \in \mathbb{R}^d$ and $y_1, \dots, y_n \in \mathbb{R}$. Let

$$\mathcal{R} = \operatorname{span}\{x_1, \dots, x_n\}, \qquad \dim(\mathcal{R}) = n,$$

let $\mathbf{X} \in \mathbb{R}^{n \times d}$ have row $i$ equal to $x_i^\top$, and set $y = (y_1, \dots, y_n)^\top$. Define

$$L_n(w) = \frac{1}{2} \sum_{i=1}^{n} \big(\langle w, x_i \rangle - y_i\big)^2.$$

Consider gradient descent

$$w_{t+1} = w_t - \eta \sum_{i=1}^{n} \big(\langle w_t, x_i \rangle - y_i\big) x_i, \qquad 0 < \eta < 2/\|\mathbf{X}\|_{\mathrm{op}}^2.$$

(a) Derive the normal equation in both forms

$$\sum_{i=1}^{n} \big(\langle w, x_i \rangle - y_i\big) x_i = 0, \qquad \mathbf{X}^\top (\mathbf{X} w - y) = 0.$$

Prove that $\dim(\mathcal{R}) = n$ is equivalent to $\mathbf{X}\mathbf{X}^\top$ being nonsingular, and deduce that the normal equation is equivalent to $\mathbf{X} w = y$.

(b) Define $w^\star = \mathbf{X}^\top (\mathbf{X}\mathbf{X}^\top)^{-1} y$. Prove that every minimizer of $L_n$ has the unique form

$$w^\star + v, \qquad v \in \mathcal{R}^\perp.$$

Use the Pythagorean theorem to prove that $w^\star$ is the unique minimum-Euclidean-norm minimizer.

(c) Let $v_0$ be the orthogonal projection of $w_0$ onto $\mathcal{R}^\perp$. Prove that the $\mathcal{R}^\perp$ component of every iterate equals $v_0$ and that

$$w_t \longrightarrow w^\star + v_0.$$

Deduce the limit for $w_0 = 0$, and give an initialization whose limit is not the minimum-norm minimizer.

Hints For (a), use the rank of $\mathbf{X}$ and the fact that a full-column-rank matrix $\mathbf{X}^\top$ is one-to-one. For (b), first substitute $w^\star$ into $\mathbf{X} w = y$. For (c), every increment belongs to $\mathcal{R}$; on $\mathcal{R}$, use an eigenbasis of $\mathbf{X}^\top \mathbf{X}$.

**Exercise 2: Logits, sigmoid probabilities, and logistic loss.**

◎ Derive binary logistic loss from a conditional probability model and distinguish the probabilistic surrogate from classification error.

Define the sigmoid function by

$$\sigma(s) = \frac{1}{1 + e^{-s}}, \qquad s \in \mathbb{R}.$$

For a score $s_w(x) = \langle w, x \rangle$ and a label $y \in \{-1, 1\}$, define

$$q_w(y \mid x) = \sigma\big(y s_w(x)\big).$$

Lecture 1 introduced a binary logit as log-odds, and Lecture 3 introduced sigmoid probabilities and log-loss fitting. This exercise reconnects those ideas for a linear score.

(a) Prove that $\sigma(s) + \sigma(-s) = 1$. Deduce that $q_w(\cdot \mid x)$ is a probability mass function on $\{-1, 1\}$ for every $x$.

(b) Prove the log-odds identity

$$\log \frac{q_w(1 \mid x)}{q_w(-1 \mid x)} = s_w(x),$$

and derive

$$-\log q_w(y \mid x) = \log\bigl(1 + e^{-y s_w(x)}\bigr).$$

Use these identities to explain each part of the terminology: why $s_w(x)$ is a *logit*, why the use of $\sigma$ makes the model *logistic*, why modeling $\mathbb{P}(Y = 1 \mid X = x)$ as a function of $x$ is called *regression*, and why the negative log-likelihood is called *logistic loss*.

(c) Fix an input $x$ and suppose $\pi = \mathbb{P}(Y = 1 \mid X = x) \in (0, 1)$. If a predictor assigns probability $q \in (0, 1)$ to label 1, its conditional expected log loss is

$$C_\pi(q) = -\pi \log q - (1 - \pi) \log(1 - q).$$

Prove that $C_\pi$ is uniquely minimized at $q = \pi$. State precisely what the identity $q = \pi$ implies when the logistic model can represent the true conditional probabilities.

(d) Show that $q_w(1 \mid x) \geq 1/2$ if and only if $s_w(x) \geq 0$. Compare the logistic training loss with the deployment loss $\mathbb{I}\{\mathrm{sign}(s_w(x)) \neq y\}$. Why is logistic loss called a surrogate loss for classification error?

Hints For (c), differentiate $C_\pi(q)$ and determine the sign of its derivative on either side of $q = \pi$. For (d), the two losses use the same signed score, but one records its magnitude and the other records only whether its sign is correct.

**Exercise 3: Why steepest-descent flow escapes to infinity.**

Complete the descent argument that makes separable logistic loss vanish along unit steepest-descent flow.

Fix a linearly separable collection $z_1, \ldots, z_n \in \mathbb{R}^d$, let

$$L_n(w) = \frac{1}{n} \sum_{i=1}^{n} \log(1 + e^{-\langle w, z_i \rangle}),$$

and let $w(t)$ solve the unit steepest-descent flow

$$\dot{w}(t) = s_p(\nabla L_n(w(t))).$$

Let $q$ be conjugate to $p$, let $\gamma_p^\star > 0$ be the maximum normalized margin, and define

$$a_i(t) = \frac{1}{n(1 + e^{\langle w(t), z_i \rangle})}, \qquad A(t) = \sum_{i=1}^{n} a_i(t).$$

Set $L_0 = L_n(w(0))$.

(a) Prove

$$\|\nabla L_n(w(t))\|_q \geq \gamma_p^\star A(t)$$

and

$$-\frac{d}{dt} L_n(w(t)) = \|\nabla L_n(w(t))\|_q.$$

(b) Prove that $L_n(w(t)) \le L_0$ and that

$$A(t) \ge e^{-nL_0} L_n(w(t)).$$

(c) Deduce the explicit bound

$$L_n(w(t)) \le L_0 \exp\bigl(-\gamma_p^\star e^{-nL_0} t\bigr).$$

Conclude that every margin $\langle w(t), z_i \rangle$ tends to infinity and that $\|w(t)\|_p \to \infty$.

Hints For (b), put $x_i = e^{-\langle w(t), z_i \rangle}$. Use $x_i \ge \log(1 + x_i)$ and $\log(1 + x_i) \le nL_n(w(t)) \le nL_0$. For (c), apply the differential inequality from parts (a)–(b), then use the fact that the loss is a finite sum of nonnegative terms.

**Exercise 4: Complete the max-margin flow proof.**

Supply the finite-sum and limiting arguments used in the max-margin flow proof.

Fix linearly separable vectors $z_1, \dots, z_n \in \mathbb{R}^d$ and let

$$L_n(w) = \frac{1}{n} \sum_{i=1}^{n} \log(1 + e^{-\langle w, z_i \rangle}).$$

Let $w(t)$ be a trajectory such that $L_n(w(t)) \to 0$ and $\|w(t)\|_p \to \infty$. Write

$$m_i(t) = \langle w(t), z_i \rangle, \quad m_{\min}(t) = \min_{i \in [n]} m_i(t), \quad a_i(t) = \frac{1}{n(1 + e^{m_i(t)})}, \quad A(t) = \sum_{i=1}^{n} a_i(t).$$

(a) Derive

$$\nabla L_n(w(t)) = -\frac{1}{n} \sum_{i=1}^{n} \frac{z_i}{1 + e^{m_i(t)}} = -\sum_{i=1}^{n} a_i(t) z_i.$$

(b) Prove that every $m_i(t) \to \infty$ and that

$$\frac{A(t)}{L_n(w(t))} \longrightarrow 1.$$

(c) Prove that, for all sufficiently large $t$,

$$m_{\min}(t) \le -\log L_n(w(t)) \le m_{\min}(t) + \log(2n).$$

Conclude that

$$-\log L_n(w(t)) = m_{\min}(t) + O(1).$$

(d) Suppose that for every $\varepsilon \in (0, \gamma_p^\star)$ and all sufficiently large $t$,

$$-\frac{d}{dt} \log L_n(w(t)) \ge (\gamma_p^\star - \varepsilon) \frac{d}{dt} \|w(t)\|_p.$$

Integrate this inequality and use part (c) to prove

$$\gamma_p(w(t)) \longrightarrow \gamma_p^\star.$$

(e) Suppose $w(t_k)/\|w(t_k)\|_p \to u$. Prove that $\|u\|_p = 1$ and

$$\min_i \langle u, z_i \rangle = \gamma_p^\star.$$

Show that $u/\gamma_p^\star$ solves

$$\min_w \|w\|_p \quad \text{subject to} \quad \langle w, z_i \rangle \geq 1 \quad (i \in [n]).$$

HINTS For (b), use the corresponding scalar asymptotic equivalence for each of the finitely many summands. For (c), use $x/2 \leq \log(1+x) \leq x$ for $x \in [0,1]$. For (e), compare an arbitrary feasible vector with its normalized direction.

**Exercise 5: The discrete steepest-descent estimate.**[*]

Prove a discrete margin estimate and distinguish unit and scaled steepest-descent stepsizes.

Fix linearly separable vectors $z_1, \dots, z_n \in \mathbb{R}^d$, let

$$L_n(w) = \frac{1}{n} \sum_{i=1}^n \log(1 + e^{-\langle w, z_i \rangle}), \qquad \gamma_p^\star = \max_{\|u\|_p \leq 1} \min_{i \in [n]} \langle u, z_i \rangle,$$

and let $q$ be conjugate to $p$. For $g \neq 0$, choose

$$s_p(g) \in \arg\min_{\|v\|_p = 1} \langle g, v \rangle,$$

so that $\|s_p(g)\|_p = 1$ and $\langle -g, s_p(g) \rangle = \|g\|_q$. Suppose that $L_n$ is $B$-smooth relative to $\|\cdot\|_p$: for all $w, \Delta$,

$$L_n(w + \Delta) \leq L_n(w) + \langle \nabla L_n(w), \Delta \rangle + \frac{B}{2} \|\Delta\|_p^2.$$

Consider the scaled discrete update

$$w_{t+1} = w_t + \eta_t \|g_t\|_q s_p(g_t), \qquad g_t = \nabla L_n(w_t).$$

Assume $\eta_t \to 0$, $L_n(w_t) \to 0$, and

$$\sum_{t=0}^\infty \eta_t \|g_t\|_q = \infty.$$

(a) Prove the one-step inequalities

$$L_n(w_{t+1}) \leq L_n(w_t) - \eta_t \|g_t\|_q^2 + \frac{B}{2} \eta_t^2 \|g_t\|_q^2,$$
$$\|w_{t+1}\|_p - \|w_t\|_p \leq \eta_t \|g_t\|_q.$$

(b) Define

$$A_t = \frac{1}{n} \sum_{i=1}^n \frac{1}{1 + e^{\langle w_t, z_i \rangle}}.$$

Prove that

$$\frac{A_t}{L_n(w_t)} \longrightarrow 1 \quad \text{and} \quad \|g_t\|_q \geq \gamma_p^\star A_t.$$

Deduce that for every $\varepsilon > 0$ and all sufficiently large $t$,

$$\log \frac{L_n(w_t)}{L_n(w_{t+1})} \geq (\gamma_p^\star - \varepsilon) \eta_t \|g_t\|_q.$$

(c) Sum the inequalities from parts (a)–(b) and prove

$$\gamma_p(w_t) \longrightarrow \gamma_p^\star.$$

(d) A unit-direction update has the form

$$w_{t+1} = w_t + \alpha_t s_p(g_t).$$

Show that the unit-direction update equals the scaled update in this exercise exactly when $\alpha_t = \eta_t \|g_t\|_q$. Deduce the following translations:

(i) gradient descent with multiplier $\beta_t$ is represented by $p = 2$, $\eta_t = \beta_t$, and unit-direction length $\alpha_t = \beta_t \|g_t\|_2$;

(ii) signed gradient descent with multiplier $\beta_t$ is represented by $p = \infty$, $\alpha_t = \beta_t$, and scaled multiplier $\eta_t = \beta_t / \|g_t\|_1$ whenever $g_t \neq 0$.

Explain why a stepsize theorem for the scaled update cannot be applied to signed gradient descent without checking the transformed multipliers.

Hints For (b), use $-\log(1-x) \geq x$ after applying the one-step loss bound, and use $\eta_t \to 0$ to absorb the quadratic term. For (c), compare both $-\log L_n(w_t)$ and $\|w_t\|_p$ with $\sum_{s<t} \eta_s \|g_s\|_q$; then use $-\log L_n(w_t) = \min_i \langle w_t, z_i \rangle + O(1)$.

**Exercise 6: A two-point population-risk reversal.**

Compute two norm-induced separators and relate their disagreement to expected population classification risk.

Let

$$z_0 = (2,1)^\top, \qquad u = (1,-3/2)^\top, \qquad v = (-1,3/2)^\top.$$

For $p \in \{2, \infty\}$, let $\widehat{w}_p$ minimize $\|w\|_p$ subject to the hard-margin constraints in an observed sample.

(a) When every observed signed feature equals $z_0$, derive

$$\widehat{w}_2 = (2/5, 1/5)^\top, \qquad \widehat{w}_\infty = (1/3, 1/3)^\top.$$

Determine the sign of the score assigned by each vector to $u$ and to $v$.

(b) Fix $\delta \in (0,1)$. Under $P_2$, let $Z = z_0$ with probability $1-\delta$ and $Z = u$ with probability $\delta$. Under $P_\infty$, replace $u$ by $v$. In either law, draw $Y$ uniformly from $\{-1,1\}$ independently of $Z$ and set $X = YZ$. For an i.i.d. sample $S_n$, prove

$$\begin{aligned} \mathbb{E}_{P_2^n}[R_{P_2}(\widehat{w}_2)] &= 0, & \mathbb{E}_{P_2^n}[R_{P_2}(\widehat{w}_\infty)] &= \delta(1-\delta)^n, \\ \mathbb{E}_{P_\infty^n}[R_{P_\infty}(\widehat{w}_\infty)] &= (1-\delta)\delta^n, & \mathbb{E}_{P_\infty^n}[R_{P_\infty}(\widehat{w}_2)] &= \delta(1-\delta)^n + (1-\delta)\delta^n. \end{aligned}$$

(c) Maximize the risk difference over $\delta$ and determine its asymptotic order as $n \to \infty$. Explain in one sentence why the calculation gives no universal population-risk ordering of the two norm biases.

Hints For (b), partition the samples into those containing only the common point, only the rare point, or both. A hard-margin solution classifies every support point that appears in its constraints.

**Exercise 7: A constant gap from private features.**

Prove that unseen private features amplify a two-dimensional norm bias into a constant expected-risk gap in proportional dimension.

Fix $n \geq 4$, set $d = n + 2$, and decompose $z = (z^{\mathrm{sh}}, z^{\mathrm{pr}}) \in \mathbb{R}^2 \times \mathbb{R}^n$. Define

$$z_0 = ((2,1)^\top, 0), \quad u_j = ((1,-3/2)^\top, ne_j), \quad v_j = ((-1,3/2)^\top, ne_j), \quad j \in [n].$$

Under $P_{2,n}$, $Z = z_0$ with probability $1/2$ and $Z = u_j$ with probability $1/(2n)$ for every $j$. Under $P_{\infty,n}$, replace $u_j$ by $v_j$. Draw $Y$ uniformly and independently from $\{-1, 1\}$ and set $X = YZ$. Let $S_n$ be an i.i.d. sample.

Let $\widehat{w}_2$ be the minimum-$\ell_2$ hard-margin separator. Let $\widehat{w}_\infty$ minimize the global $\ell_\infty$ norm and then minimize the Euclidean norm among the max-norm minimizers. Let $G_n = \{z_0 \text{ appears in } S_n\}$.

(a) Prove that on $G_n$ the shared coordinates of $\widehat{w}_\infty$ equal $(1/3, 1/3)^\top$. Exhibit feasible private parameter coefficients for every observed rare identity under each population, and prove that the coefficient associated with every unobserved identity is zero.

(b) Set $w_2^\star = (2/5, 1/5)^\top$. Construct a feasible Euclidean comparison vector and prove that, on $G_n$,

$$\|\widehat{w}_2^{\mathrm{sh}} - w_2^\star\|_2^2 \leq \frac{121}{100n}.$$

Deduce that the signs assigned by the shared coordinates to the rare points agree with those in the two-dimensional example for all sufficiently large $n$.

(c) For a fixed rare identity $j$, compute the probability that $j$ is absent from $S_n$ while $G_n$ occurs. Sum over $j$ and prove that the favored selector has expected risk tending to zero while the disfavored selector has expected risk tending to

$$\frac{1}{2}e^{-1/2}.$$

Prove this conclusion under both $P_{2,n}$ and $P_{\infty,n}$, with the roles of the selectors reversed.

(d) State precisely which aspects of the learning problem change with $n$. Does the result prove inconsistency for a fixed finite-dimensional population law?

Hints For (a), the common constraint and $\|w\|_\infty \leq 1/3$ force equality in $2w_1 + w_2 \leq 3\|w\|_\infty$. For (b), use at most $n$ private parameter coefficients, each of magnitude at most $11/(10n)$. For (c), subtract the event that neither the common point nor identity $j$ appears from the event that identity $j$ does not appear.

**Exercise 8: Equal margins preserve a signed-gradient ray.**[*]

Recognize when coordinate normalization confines an adaptive method to one parameter ray.

Let $\mathbf{X} \in \mathbb{R}^{n \times d}$ have row $i$ equal to $x_i^\top$, let $y \in \{-1, 1\}^n$, and define

$$s = \mathrm{sign}(\mathbf{X}^\top y).$$

Assume $\mathbf{X}s = cy$ for some $c > 0$.

(a) For a differentiable margin loss $L(w) = \sum_{i=1}^n \ell(y_i \langle w, x_i \rangle)$, prove that

$$\nabla L(\alpha s) = \ell'(c\alpha)\mathbf{X}^\top y.$$

When $\ell' < 0$, prove by induction that signed gradient descent initialized at zero remains on the ray $\{\alpha s : \alpha \geq 0\}$.

(b) For the squared loss $Q(w) = \frac{1}{2}\|\mathbf{X}w - y\|_2^2$, prove

$$\nabla Q(\alpha s) = (c\alpha - 1)\mathbf{X}^\top y.$$

Explain why an adaptive update that divides each nonzero gradient coordinate by a matching coordinatewise magnitude also remains on the ray.

(c) Explain why replacing the denominator $|g_j|$ by $|g_j| + \epsilon$ for fixed $\epsilon > 0$ generally breaks the exact ray calculation as the gradient vanishes. Contrast the consequences for a finite least-squares interpolant and for logistic loss on separable data.

**Exercise 9: Early stopping as a spectral filter.**[*]

Diagonalize least-squares gradient descent and interpret stopping time as eigendirection-dependent regularization.

Let $H = \mathbf{X}^\top\mathbf{X}$, $b = \mathbf{X}^\top y$, $w_0 = 0$, and

$$w_{t+1} = (I - \eta H)w_t + \eta b, \qquad 0 < \eta < 2/\|H\|_{\mathrm{op}}.$$

Let $H = \sum_{j=1}^d \lambda_j q_j q_j^\top$ be an orthonormal eigendecomposition.

(a) Prove that

$$w_t = \sum_{j:\lambda_j>0} \frac{1 - (1 - \eta\lambda_j)^t}{\lambda_j}\langle q_j, b\rangle q_j.$$

Justify why the coordinates with $\lambda_j = 0$ vanish.

(b) Define $g_t(\lambda) = [1 - (1 - \eta\lambda)^t]/\lambda$. Show that $g_t(\lambda) \to 1/\lambda$ for every positive eigenvalue. For $0 \le \eta\lambda \le 1$, prove

$$1 - e^{-\eta\lambda t} \le 1 - (1 - \eta\lambda)^t \le \eta\lambda t.$$

Use these bounds to identify the transition scale in $\lambda$.

(c) Ridge regression uses the filter $g_\rho(\lambda) = 1/(\lambda + \rho)$. Compare the limiting behavior of $g_t$ and $g_\rho$ when $\lambda$ is much larger or much smaller than $1/(\eta t)$ and $\rho$, respectively. State the sense in which early stopping regularizes small-eigenvalue directions.

Hints For (a), unroll the affine recursion and sum a geometric series in each eigendirection. For (b), use $1 - x \le e^{-x}$ and Bernoulli's inequality.

## References

Lukas Balles and Philipp Hennig. Dissecting Adam: The sign, magnitude and variance of stochastic gradients. Proceedings of the 35th International Conference on Machine Learning, 2018. https://proceedings.mlr.press/v80/balles18a.html.

Guy Blanc, Neha Gupta, Gregory Valiant, and Paul Valiant. Implicit regularization for deep neural networks driven by an Ornstein–Uhlenbeck like process. Proceedings of the 33rd Conference on Learning Theory, 2020. https://proceedings.mlr.press/v125/blanc20a.html.

Laurent Dinh, Razvan Pascanu, Samy Bengio, and Yoshua Bengio. Sharp minima can generalize for deep nets. Proceedings of the 34th International Conference on Machine Learning, 2017. https://proceedings.mlr.press/v70/dinh17b.html.

Suriya Gunasekar, Jason D. Lee, Daniel Soudry, and Nathan Srebro. Characterizing implicit bias in terms of optimization geometry. Proceedings of the 35th International Conference on Machine Learning, 2018. https://proceedings.mlr.press/v80/gunasekar18a.html.

Jeff Z. HaoChen, Colin Wei, Jason D. Lee, and Tengyu Ma. Shape matters: Understanding the implicit bias of the noise covariance. Proceedings of the 34th Conference on Learning Theory, 2021. https://proceedings.mlr.press/v134/haochen21a.html.

Chen Fan and Csaba Szepesvári. On the two faces of Adam in separable linear classification. arXiv preprint arXiv:2609.33904, 2026. https://arxiv.org/abs/2609.33904.

Chen Fan, Mark Schmidt, and Christos Thrampoulidis. Implicit bias of spectral descent and Muon on multiclass separable data. Advances in Neural Information Processing Systems, 38, 2025. https://arxiv.org/abs/2502.04664.

Zhiyuan Li, Tianhao Wang, and Sanjeev Arora. What happens after SGD reaches zero loss?—A mathematical framework. International Conference on Learning Representations, 2022. https://openreview.net/forum?id=siCt4xZn5Ve.

Stephan Mandt, Matthew D. Hoffman, and David M. Blei. Stochastic gradient descent as approximate Bayesian inference. Journal of Machine Learning Research, 18(134):1–35, 2017. https://www.jmlr.org/papers/v18/17-214.html.

Scott Pesme, Loucas Pillaud-Vivien, and Nicolas Flammarion. Implicit bias of SGD for diagonal linear networks: A provable benefit of stochasticity. Advances in Neural Information Processing Systems, 34, 2021. https://proceedings.neurips.cc/paper/2021/hash/f4661398cb1a3abd3ffe58600bf11322-Abstract.html.

Robin M. Schmidt, Frank Schneider, and Philipp Hennig. Descending through a crowded valley—benchmarking deep learning optimizers. Proceedings of the 38th International Conference on Machine Learning, 2021. https://proceedings.mlr.press/v139/schmidt21a.html.

Prabhu Teja Sivaprasad, Florian Mai, Thijs Vogels, Martin Jaggi, and François Fleuret. Optimizer benchmarking needs to account for hyperparameter tuning. Proceedings of the 37th International Conference on Machine Learning, 2020. https://proceedings.mlr.press/v119/sivaprasad20a.html.

Daniel Soudry, Elad Hoffer, Mor Shpigel Nacson, Suriya Gunasekar, and Nathan Srebro. The implicit bias of gradient descent on separable data. Journal of Machine Learning Research, 19(70):1–57, 2018. https://www.jmlr.org/papers/v19/18-188.html.

Bhavya Vasudeva, Jung Whan Lee, Vatsal Sharan, and Mahdi Soltanolkotabi. The rich and the simple: On the implicit bias of Adam and SGD. Advances in Neural Information Processing

Systems, 38, 2025. https://arxiv.org/abs/2505.24022.

Bohan Wang, Qi Meng, Huishuai Zhang, Ruoyu Sun, Wei Chen, Zhi-Ming Ma, and Tie-Yan Liu. Does momentum change the implicit regularization on separable data? Advances in Neural Information Processing Systems, 2022.

Ashia C. Wilson, Rebecca Roelofs, Mitchell Stern, Nathan Srebro, and Benjamin Recht. The marginal value of adaptive gradient methods in machine learning. Advances in Neural Information Processing Systems, 30, 2017. https://papers.nips.cc/paper_files/paper/2017/hash/81b3833e2504647f9d794f7d7b9bf341-Abstract.html.

Yuan Yao, Lorenzo Rosasco, and Andrea Caponnetto. On early stopping in gradient descent learning. Constructive Approximation, 26:289–315, 2007.

Chenyang Zhang, Difan Zou, and Yuan Cao. The implicit bias of Adam on separable data. Advances in Neural Information Processing Systems, 37, 2024.

Yushun Zhang, Congliang Chen, Tian Ding, Ziniu Li, Ruoyu Sun, and Zhi-Quan Luo. Why transformers need Adam: A Hessian perspective. Advances in Neural Information Processing Systems, 37, 2024.